Chemical Physics Letters 464 (2008) 160–165

Contents lists available at ScienceDirect

Chemical Physics Letters

journal homepage: www.elsevier.com/locate/cplett

Molecular dynamics simulation of metal coating on single-walled carbon nanotube

Shuhei Inoue *, Yukihiko Matsumura

Department of Mechanical System Engineering, Hiroshima University, 1-4-1 Kagamiyama, Higashi-Hiroshima-shi, Hiroshima 739-8527, Japan

ARTICLE INFO

Article history:
Received 25 July 2008
In final form 8 September 2008
Available online 11 September 2008

ABSTRACT

Behaviors of various metals coating on single-walled carbon nanotubes are simulated by molecular dynamics. Some of the potential parameter sets are derived by DFT calculations. The results indicate that each metal species can be smoothly coated on an isolated carbon nanotube, depending on the coating condition; however, continuous coating may not always be possible. The equilibrium position on the carbon nanotube is fixed; therefore, the coating is discontinuous for a large sized atom to reduce the distortion. The diffusion rate of the metal atoms is expressed in terms of the ratios of the binding energies of metal–metal and metal–carbon bonds.

1. Introduction

Carbon nanotubes [1] have been considered one of the most fascinating materials ever since their discovery. There are three types of carbon nanotubes, namely, multi-walled, double-walled [2], and single-walled [3]. Among them, single-walled carbon nanotubes (SWCNTs) in particular have attracted considerable scientific and commercial interest. In the last 20 years, significant efforts have been made to produce them on a macroscopic scale; therefore, some prominent techniques such as high-pressure CO conversion (HiPco) [4], alcohol catalytic chemical vapor deposition (ACCVD) [5], and super-growth [6] techniques have been developed. However, the growth mechanism of the SWCNTs is still unclear, and only several related ideas have been proposed [7–13] on the basis of experimentally and theoretically obtained data. On the other hand, due to their important applications, evaporation of metals on vertically aligned SWCNT [14] film and metal coating on carbon nanotubes [15] have been studied extensively. These techniques are expected to enhance the functionalities of carbon nanotubes. For example, SWCNT may work as a quantum wire in itself, but one-third of the SWCNTs produced are metallic in nature while others are semiconducting. At present we have not been able to control its electric properties, which are determined by its chirality. A semiconducting SWCNT is not suitable for its use as a quantum wire and the metallic SWCNT is not suitable as a diode. In contrast, by coating a desired metal species on the SWCNT, we can control its electrical properties. Moreover, we can maintain its diameter to a small value by applying a single layer of the metal species. It should be noted that the physical strength of the coated nanotube will be comparable to that of a pure SWCNT. Both of these techniques (deposition and coating) are closely related to conjugation between the carbon nanotube and the metal, and their adhesion determines the properties of the resulting SWCNT. According to Zhang et al., titanium and nickel show good conjugation with carbon nanotubes, whereas gold and aluminum do not. Their binding energies were discussed by considering their adhesion behavior with carbon nanotubes.

In this study, we have simulated various metal coating processes on isolated and bundled SWCNTs by using molecular dynamics simulation. Some of the parameter sets of metal–metal and metal–carbon potentials are derived by fitting their binding energies with density functional theory (DFT) calculations, and the Brenner potential [16] is used for the carbon–carbon interaction. The results of this study indicate that the coating behavior cannot be simply explained by the strength of the interaction between the metal and the carbon nanotube, which is expressed as a potential depth. Even a gold atom, which does not yield a smooth coating on the carbon nanotube experimentally, can be coated smoothly under suitable conditions; however, continuous coating is difficult to achieve.

2. Methods

The Brenner potential was applied to the carbon–carbon interaction and the classical many-body potential [17] was applied to the metal–metal and carbon–metal interactions as a function of the bond number. The parameter sets for the nickel–nickel, carbon–nickel, iron–iron, and carbon–iron interactions were obtained from the results of Shibuta and Maruyama [18]. Whereas, the parameter sets for the gold–gold, carbon–gold, titanium–titanium, and carbon–titanium ones were derived by density functional theory (DFT) calculations. GAUSSIAN 03 [19] and Becke's three-parameter exchange functional with the Lee–Yang–Parr correlation functional (B3LYP) [20,21] were used in this study. The Los Alamos effective core potential plus DZ (LANL2DZ) [22] was used as the basis set.

* Corresponding author. Fax: +81 82 424 5923.
E-mail address: shu18@hiroshima-u.ac.jp (S. Inoue).

0009-2614/$ - see front matter © 2008 Elsevier B.V. All rights reserved.
doi:10.1016/j.cplett.2008.09.014

Since the method for deriving the parameter sets is identical to that used in the above-mentioned paper [18], we briefly explain it here. First, we assume that the M_x and MC_x clusters have a symmetrical structure; this implies that all bond lengths are equal. Then, we calculate their total energies. The binding energy is calculated by subtracting the total isolated atom energies from the total energy and dividing by the number of bonds, as shown in Eq. (1):

$$De = (E_{\min}^{\text{total}} - E_{\text{m,min}}^{\text{isolated}} - N_c \cdot E_{\text{c,min}}^{\text{isolate}})/N_b \quad (1)$$

where $E_{\min}^{\text{total}}$ denotes the total energy of a certain spin state, $E_{\text{m,min}}^{\text{isolated}}$ is the isolated energy of the metal, N_c is the coordination number of carbon, $E_{\text{c,min}}^{\text{isolate}}$ is the isolated energy of carbon, and N_b is the bond number. In each case, several spin states are calculated and their minimum values corresponding to a specific distance are employed for the fitting. The clusters usually attain various spin states, depending on the bond length; we employed the one having the minimum bond length. Table 1 shows all parameter sets expressed in Eqs. (2)–(9).

$$E = V_R - V_A \quad (2)$$

$$V_R = \frac{D_e S}{S-1}\exp\{-\beta\sqrt{2S}(r - R_e)\} \quad (3)$$

$$V_A = B^* \frac{D_e S}{S-1}\exp\{1 + b(N^C - 1)\}^{\delta} \quad (4)$$

$$D_e = D_{e1} + D_{e2}\exp\{-C_D(N^M - 1)\} \quad (5)$$

$$R_e = R_{e1} - R_{e2}\exp\{-C_R(N^M - 1)\} \quad (6)$$

$$f(r) = \begin{cases} 1 & (r < R_1) \\ 0.5 \cdot \left(1 + \cos\frac{r-R_1}{R_2-R_1}\pi\right) & (R_1 < r < R_2) \\ 0 & (R_2 < r) \end{cases} \quad (7)$$

$$N_i^C = 1 + \sum_{\text{carbon}} f(r_{ik}) \quad (8)$$

$$N_i^M = 1 + \sum_{\text{metal}} f(r_{ik}) \quad (9)$$

In the above equations, r denotes the distance between two atoms, and V_R and V_A denote the Morse-type potential for the repulsion and attraction terms, respectively. R_e denotes the equilibrium bond length, and D_e is the potential depth at $r = R_e$. S represents the ratio of the effective repulsion to attraction. N_i^C and N_i^M are the coordination numbers derived from the cut-off function $f(r)$.

The dimensions of the calculated system are 60 Å × 100 Å × 100 Å, and a periodic boundary condition is applied in each direction. As shown in Fig. 1, an isolated SWCNT is 60 Å in length with (5,5) chirality; both its ends are fixed, and the next two layers work to control its temperature. Before coating this carbon nanotube with a metal, it is annealed at 300 K by velocity scaling technique. The molecules of the coating metal are expressed as M_{13} clusters; this expression is suitable for actual experiment because in the conventional metal evaporation process, the average metal particle size is approximately a few angstroms in diameter. This metal cluster is also fully annealed at 1200–1400 K; the annealing temperature is clearly higher than their melting temperature but less than their boiling temperature. The melting temperatures in the bulk form expressed by these potential parameters are approximately 1800–2000 K; however, in this Letter, the metal clusters under study are too small to exhibit bulk properties. In order to achieve continuous metal evaporation coating, the fully annealed metal clusters are distributed at appropriate distances (15–20 Å) and made to collide with the carbon nanotube at a low evaporation energy of 10 meV or 30 meV.

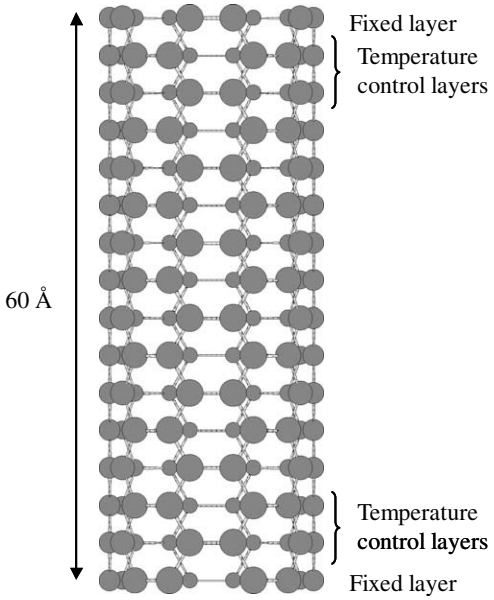

Fig. 1. Isolated single-walled carbon nanotube. Both the ends are fixed layer and following two layers work to control the temperature.

3. Results and discussion

Fig. 2 shows the simulation result of continuous metal evaporation coating ((a) Ti, (b) Fe, (c) Ni, and (d) Au). In this simulation, 24 M_{13} clusters were gently collided with one SWCNT. The impact direction was perpendicular to the axis of the carbon nanotube, and at each impact point, about four clusters collided simulta-

Table 1
Potential parameters

Atom	S	β (Å^{-1})	D_{e1} (eV)	D_{e2} (eV)	C_D	R_{e1} (Å)	R_{e2} (Å)	C_R	R_1 (Å)	R_2 (Å)
Fe–Fe[a]	1.3	1.2173	0.4155	0.8392	0.8730	2.627	0	–	2.7	3.2
Ni–Ni[a]	1.3	1.5700	0.4217	1.0144	0.8268	2.4934	0.1096	0.3734	2.7	3.2
Ti–Ti	1.3	2.331	0.6500	0.2001	0.3700	3.819	2.411	0.2357	2.7	3.2
Au–Au	1.3	1.7500	0.5290	1.3510	1.5251	3.3043	0.7573	0.2939	2.9	3.5

Atom	De (eV)	S	β (Å^{-1})	R_e (Å)	R_1 (Å)	R_2 (Å)	b	δ
Fe–C[a]	3.3249	1.3	1.5284	1.7304	2.7	3.0	0.0656	−0.4279
Ni–C[a]	2.4673	1.3	1.8706	1.7628	2.7	3.0	0.0688	−0.5351
Ti–C	3.624	1.3	1.466	1.800	2.7	3.0	0.0600	−0.5000
Au–C	2.1840	1.3	2.0745	1.9030	2.9	3.3	0.0970	−0.5350

[a] These values are referred to Shibuta and Maruyama.

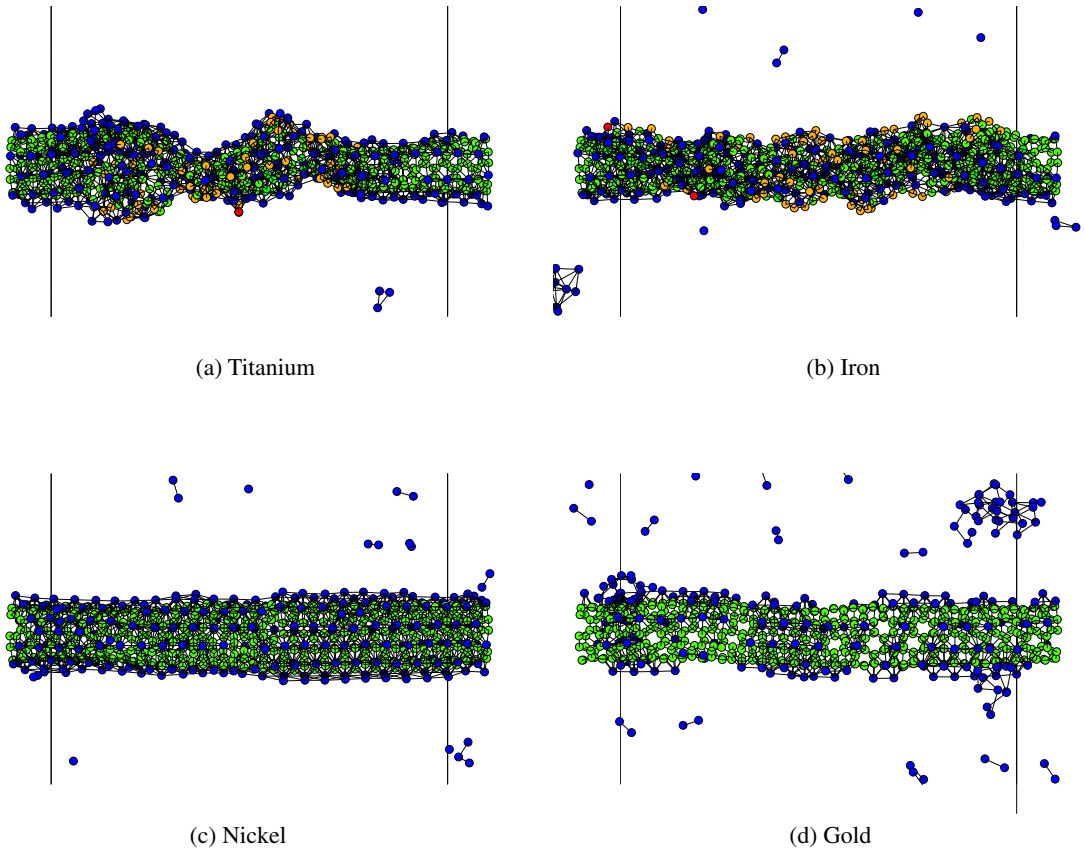

Fig. 2. Continuous metal evaporation. Blue is metal atom, green is carbon atom with three bonds (sp^2), orange is carbon atom with two bonds (one dangling bond), and red is carbon atom with one bond (two dangling bonds). (For interpretation of the references to color in this figure legend, the reader is referred to the web version of this article.)

neously. In case of titanium and iron clusters (Fig. 2a and b), the metal atoms seemed to firmly combine with carbon atoms; thus, the metal atoms entered the carbon nanotube and distorted its structure. The strong interaction between the metal atoms and carbon caused the structural deformation of the nanotube; moreover, the continuous impact in a short time for reducing the calculation load (10 ps/layer; usually 1–250 ms/layer in evaporation method for pure gold in experiment) resulted in unrealistic phenomena. In the case of nickel clusters (Fig. 2c), the nickel atoms smoothly and seamlessly covered the carbon nanotube. The equilibrium position of the nickel atoms coincided with the center of the hexagonal carbon network. When the first nickel cluster collided with the carbon nanotube, a grain structure was temporarily formed; however, the nickel atoms immediately found a stable position and moved into it. Once they reached the equilibrium position, they remained stationary at this temperature. Next, the second cluster reached the surface, acquired a grain structure instantly, and then moved to the most stable site. When all the clusters reached the surface, the equilibrium position on the carbon network was saturated; therefore, the nickel clusters formed a second metal layer on the carbon nanotube. Even at this stage, the nickel atoms did not form a grain structure but formed a smooth and seamless layer. Fig. 2d shows the result of gold cluster coating. According to Zhang et al., gold atoms form a grain structure and exhibit a highly discontinuous coating; however, according to our simulation, the gold atoms can be coated smoothly but discontinuously. The gold atoms initially formed a grain structure, as reported by Zhang et al.; this was because the gold clusters were accidentally concentrated in the same area on the carbon nanotube. This indicates that if the evaporation rate decreases or the experiment is conducted under a higher vacuum condition, the formation of a grain structure can be avoided. Zhang et al. explained this result in terms of the weak interaction between the gold atoms and the SWCNT. However, according to our DFT calculations, the binding energy of the Au–C bond is not low; on the contrary, it is slightly larger than the binding energy of the Au–Au bond. The value of the binding energy is not considered to be significant; however, the ratio of the binding energies, i.e., E_{M-C}/E, should be substantial. Because under this condition each atom has many coordination number, the values of this ratio for titanium, iron, nickel, and gold are 2, 3, 1.5 (approximately), and 1 (approximately), respectively. Thus, in the case of titanium and iron coating, the carbon atoms experience an outward pull and the nanotube structure gets deformed. In the case of nickel, a very smooth coating is achieved. On the other hand, in the case of gold, though the Au–C interaction is slightly stronger than the Au–Au interaction, a grain structure is formed. In some areas, the gold atoms are deposited smoothly but not seamlessly. The reason for this phenomenon is attributed to the equilibrium bond length. As mentioned above, the most stable site for the first layer metal atoms is the center of the hexagonal carbon network, of whose diameter is 2.5 Å. Coincidently, the equilibrium bond lengths of nickel and iron are comparable, but that of gold is slightly greater (2.6–3.3 Å, depending on the coordination number). The gold atoms must have a shorter bond length so that they can get accommodated in the stable site of the carbon nanotube, thereby creating a discontinuous coating that reduces the distortion energy. Thus, even gold atoms can be coated smoothly, provided the distances between them are sufficient to reduce the distortion for each fragment of coating (in our simulation, the fragment of coatings is approximately 10–15 nm in length).

Due to the strong C–Ti and C–Fe interactions, the structure of the carbon nanotube is distorted under a high coating rate in our

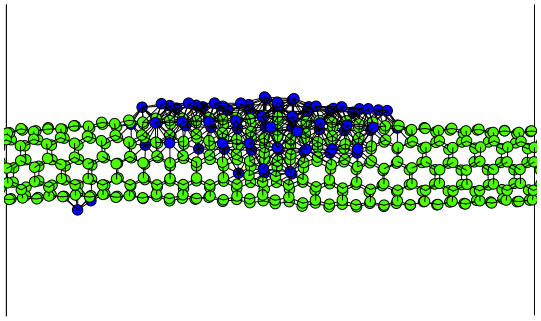

(a) Sequential Fe coating. Totally six Fe13 clusters collide.

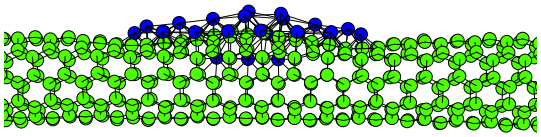

(b) Sequential Ti coating. Totally three Ti13 clusters collide.

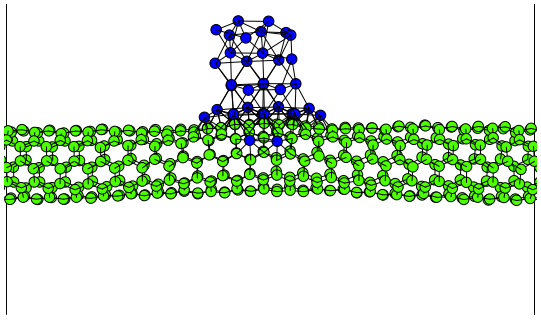

(b) Sequential Au coating. Totally three Au13 clusters collide.

Fig. 3. Sequential impacts of Fe, Ti, and Au cluster on the carbon nanotube surroundings with enough annealing duration after every impact.

simulation. In order to confirm this, a lower coating rate is applied and the results are examined. In this case, each M_{13} cluster collides with the center of the carbon nanotube in a sequence. For the fully annealing, this sequential impact took an enough interval. Fig. 3 shows this sequential impact of the metal clusters on the carbon nanotube. A full annealing duration for each impact step results in a smooth and continuous coating and no defects are observed in the carbon nanotube. A schematic diagram of the iron cluster impact is shown in Fig. 3a. Similar to the nickel atom, the iron atom finds a stable position and moves into it. However, in this simulation, because each cluster reaches almost the same position, all the iron atoms do not spread over the surface but form a second layer. This can occur in the nickel system as well. When too many clusters arrive at the same point, each atom seeks the stable site and tends to move into it, but the temperature reduces before the diffusion is completed. As a result, the iron atoms form a second layer. A similar behavior is observed in titanium coating, as shown in Fig. 3b. However, in the case of titanium clusters, when the impact energy is small, a different phenomenon is observed. In our simulation, first three clusters were able to reach the surface even at a low evaporation energy, but the next cluster could not, as shown in Fig. 4. This can be attributed to the difference in the equilibrium bond lengths. According to Eq. (6), if the number of coordinates is sufficient, the equilibrium bond length must be equal to R_{e1} for the metal–metal potential and the metal–carbon equilibrium bond length is simply determined as a function of R_e (Table 1). A comparison reveals that the difference in this value for the titanium coating system is larger than those for the iron coating system. This is because if there is a titanium layer on the carbon nanotube, the cluster having a small impact energy cannot overcome the repulsive energy. Thus, the cluster is reflected before it is attracted to the carbon atoms. This proves that at a high evaporation energy (e.g., 1 eV), the titanium cluster can arrive at the surface and produce a smooth coating. This might be a reason why the titanium coating is smoother than the nickel coating in the experimental results [15]. In the case of gold coating, as shown in Fig. 3c, the first cluster was able to spread over the surface but the second and the third could not; therefore, they formed a grain structure. This indicates that if the gold cluster reaches the same place, as in the case of the experiment with a high deposition rate, the grain formation is not avoidable, as inferred from Fig. 2d. From the point of wettability the contact angle is closely related to the wettability, which

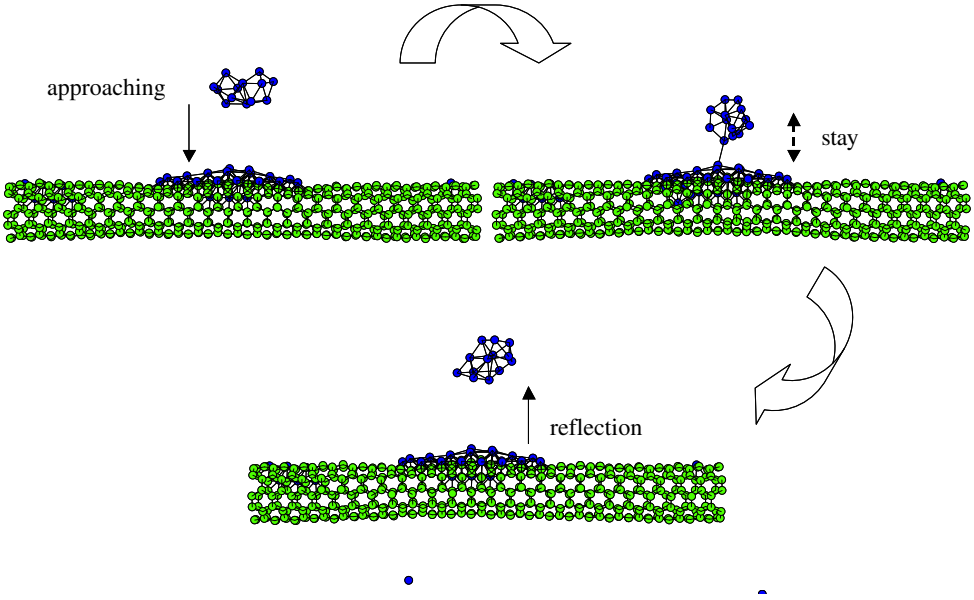

Fig. 4. A sequential coating with small evaporation energy. First, the titanium cluster approaches the SWCNT, secondly it stays above the surface for a while, and finally it is reflected.

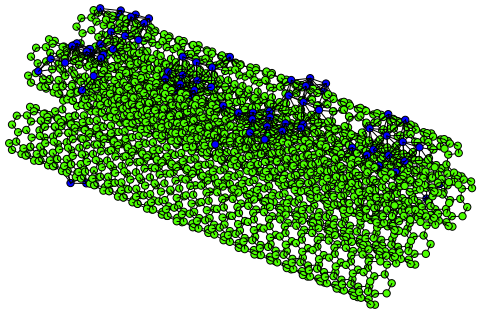

(a-1) coating by first nickel clusters

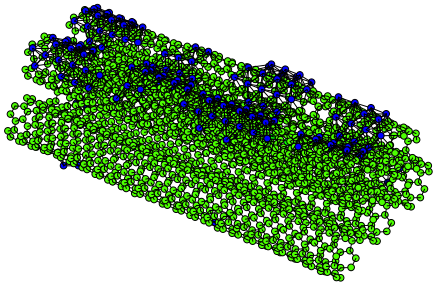

(a-2) coating by second nickel clusters

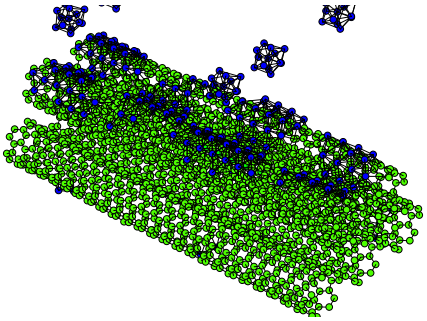

(a-3) coating by third nickel clusters

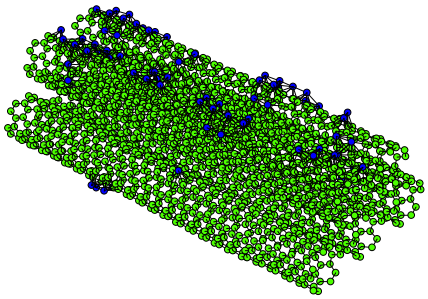

(b-1) coating by first gold clusters

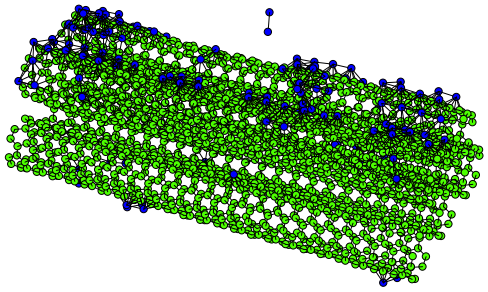

(b-2) coating by second gold clusters

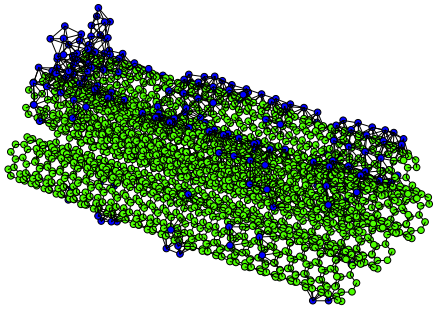

(b-3) coating by third gold clusters

Fig. 5. Sequential coating of nickel (a) and gold (b) clusters on one bundle single-walled carbon nanotube.

is well explained by solid–liquid affinity ($\varepsilon_{sl}/\varepsilon_{l}$) [23]. According to their results the contact angle tends to become larger as the solid–liquid affinity becomes smaller meaning that the gold cluster tends to form a grain structure.

With regard to quantum wires, coating a bundle of SWCNTs coated with a metal can also act as a nanowire. Fig. 5 shows sequential metal coating ((a) nickel, (b) gold) on a bundle of SWCNTs. The distances of each SWCNT are employed the value of the distance of graphite layer. In the case of coating the bundle, nickel atoms cover the surface smoothly. It is speculated that it is difficult to cover the interstitial site smoothly because the clearance is not sufficient. However, the nickel atoms can penetrate to a distance equal to half of the depth of the interstitial site. In the interstitial site, the coating has multiple layers, but does not show a grain structure. In contrast, the gold atoms form a more grained structure on the bundled SWCNTs than on the isolated SWCNT. In bundle coating, the gold atoms condense in the interstitial site, which becomes a seed for grain nucleation. Our simulation results are almost in agreement with the experimental results, except in the case of iron coating. It is speculated that because the iron atoms have a strong interaction with carbon, they locally interfere with the carbon–carbon bond or might be absorbed into the SWCNT, which triggers grain nucleation. In fact, in our simulation performed at a higher coating rate, the iron atom breaks the SWCNT structure, yielding a discontinuous surface that can result in a grain structure.

4. Conclusion

Some of the potential parameter sets have been derived by DFT calculations and different metals are coated on SWCNTs. It is observed that titanium, iron, and nickel can form a smooth and continuous coating, but gold forms a discontinuous coating. The possible reason for this is that the energy gain in the case of gold, i.e., $E_{Au-C} - E_{Au-Au}$, is not as large as that of the other metals. Before the surface diffusion is completed, the gold atoms adhere to the nanotube; this results in a grain structure. Further, the stable site for the metal atoms on the carbon nanotube is the center of the hexagonal carbon network. However, the size of this site is too small to accommodate large atoms such as gold. Thus, the gold atoms get deposited on the nanotube at sufficient distances in each fragment of coatings to reduce its distortion, which leads to a discontinuous coating.

The results generated by our simulation are in good agreement with the experimental results, except in the case of iron coating. The reason for this disagreement has not been explained. However, it is speculated that the strong Fe–C interaction is responsible for it.

References

[1] S. Iijima, Nature 354 (1991) 56.
[2] M.S. Dresselhaus, G. Dresselhaus, R. Saito, Carbon 33 (1995) 883.
[3] S. Iijima, T. Ichihashi, Nature 363 (1993) 603.
[4] H.J. Dai, A.G. Rinzler, P. Nikolaev, A. Thess, D.T. Colbert, R.E. Smalley, Chem. Phys. Lett. 260 (1996) 471.
[5] S. Maruyama, R. Kojima, Y. Miyauchi, S. Chiashi, M. Kohno, Chem. Phys. Lett. 360 (2002) 229.
[6] K. Hata, D.N. Futaba, K. Mizuno, T. Namai, M. Yumura, S. Iijima, Science 306 (2004) 1362.
[7] M. Yudasaka, R. Yamada, S. Iijima, J. Phys. Chem. B 103 (1999) 6224.
[8] H. Kataura, Y. Kumazawa, Y. Maniwa, Y. Ohtsuka, R. Sen, S. Suzuki, Y. Achiba, Carbon 38 (2000) 1691.
[9] M. Yudasaka, Y. Kasuya, F. Kokai, K. Takahashi, M. Takizawa, S. Bandow, S. Iijima, Appl. Phys. A 74 (2002) 377.
[10] J.B. Nagy et al., J. Nanosci. Nanotechnol. 4 (2004) 326.
[11] S. Inoue, Y. Kikuchi, Chem. Phys. Lett. 410 (2005) 209.
[12] Y. Shibuta, S. Maruyama, Chem. Phys. Lett. 382 (2003) 381.
[13] X. Fan, R. Buczko, A.A. Puretzky, D.B. Geohegan, J.Y. Howe, S.T. Pantelides, S.J. Pennycook, Phys. Rev. Lett. 91 (2003) 145501.
[14] K. Ishikawa, H.M. Duong, J. Shiomi, S. Maruyama, Extended Abstracts, ASME-JSME Thermal Eng., 2007, HT2007-32783.
[15] Y. Zhang, N.W. Franklin, R.J. Chen, H.J. Dai, Chem. Phys. Lett. 331 (2000) 35.
[16] D.W. Brenner, Phys. Rev. B 42 (1990) 9458.
[17] Y. Yamaguchi, S. Maruyama, Euro. Phys. J. D 9 (1999) 385.
[18] Y. Shibuta, S. Maruyama, Comput. Mat. Sci. 39 (2007) 842.
[19] M.J. Frisch et al., Gaussian 03, Revision C.02, Gaussian, Inc., Wallingford, CT, 2004.
[20] A.D. Beche, J. Chem. Phys. 98 (1993) 5648.
[21] C.T. Lee, W.T. Yang, R.G. Parr, Phys. Rev. B 37 (1998) 785.
[22] P.J. Hay, W.R. Wadt, J. Chem. Phys. 82 (1985) 270.
[23] S. Maruyama, T. Kurashige, S. Matsumoto, Y. Yamaguchi, T. Kimura, Micro. Thermophys. Eng. 2 (1998) 49.